GYNECOLOGIC ONCOLOGY 52, 31–38 (1994)

Fluorescence Spectroscopy: A Diagnostic Tool for Cervical Intraepithelial Neoplasia (CIN)

N. RAMANUJAM, M.S.,* M. F. MITCHELL, M.D.,† A. MAHADEVAN, M.S.,* S. THOMSEN, M.D.,‡ E. SILVA, M.D.,‡ AND R. RICHARDS-KORTUM, PH.D.*

*Biomedical Engineering Program, University of Texas, Austin, Texas 78712; and †Department of Gynecology and ‡Department of Pathology, University of Texas M.D. Anderson Cancer Center, Houston, Texas 77030

Received June 6, 1993

A spectroscopic system incorporating a pulsed nitrogen laser, an optical fiber probe, and an optical multichannel analyzer was utilized to record fluorescence spectra of the intact cervix at colposcopy. Spectra were obtained from 66 colposcopically normal areas and 49 histologically abnormal areas (5 pathologic inflammation, 21 HPV infection, 9 CIN I, 10 CIN II, and 4 CIN III) in 28 patients. The resulting spectra could be used to differentiate histologically abnormal tissues from colposcopically normal tissues with a sensitivity, specificity, and positive predictive value of 92, 90, and 88%. Furthermore, CIN could be differentiated from nonneoplastic abnormal tissues with a sensitivity, specificity, and positive predictive value of 87, 73, and 74%. These results suggest that laser-induced fluorescence can be used in the recognition and differential diagnosis of CIN at colposcopy.

INTRODUCTION

It is estimated that the mortality of cervical carcinoma will rise by 20% in the years 2000–2004 unless further improvements in current screening and diagnostic techniques are made [1]. A false-negative error rate of 20–30% is associated with cytologic techniques used for initial screening of CIN [2,3]. An abnormal pap smear is followed by colposcopy, which has a limited predictive value even in experienced hands. Therefore, biopsy and histologic analysis are necessary for accurate diagnosis of CIN [4]. A method to improve the predictive value of colposcopy, particularly for less experienced practitioners, could save patients from multiple biopsies and allow faster, more effective patient diagnosis and treatment. For example, if the physician had a positive diagnosis for CIN at colposcopy, the loop electrosurgical procedure (LEEP) could be performed, allowing patients to be diagnosed and treated in one visit.

Laser-induced fluorescence spectroscopy is a technique which has the potential to improve the predictive value of colposcopy. Many groups have shown that low-power laser illumination can induce endogenous tissue fluorescence and that the spectral characteristics of the resulting fluorescence depend upon the chemical and morphologic composition of tissue [5–8]. Furthermore, spectroscopic differences can be used to differentiate diseased and normal tissues. Fluorescence spectra have been measured *in vivo* in real time to detect neoplastic tissues in a variety of organ systems [5–7]. Lam *et al.* demonstrated that the sensitivity of fluorescence bronchoscopy was significantly greater than that of conventional white-light bronchoscopy in detecting dysplasia and carcinoma *in situ* using ratios of red to green autofluorescence at 442 nm excitation [5]. In the gastrointestinal tract, autofluorescence was used to distinguish adenomatous polyps from normal colon and hyperplastic polyps [6,7]. Cothren *et al.* [6] developed an algorithm based on fluorescence intensities at 460 and 680 nm emission (370 nm excitation) to differentiate adenomas from nonadenomas with a positive predictive value, sensitivity, and specificity of 94, 100, and 97%. Schomacker *et al.* [7] were able to differentiate adenomatous polyps from hyperplastic polyps (337 nm excitation) with a positive predictive value, sensitivity, and specificity of 86, 86, and 80%, using scores developed from multivariate linear regression analysis.

In vitro excitation–emission spectra of normal and abnormal cervical tissue from patients with suspected CIN show that, at excitation wavelengths of 330, 350, and 450 nm, the fluorescence of histologically abnormal tissue is significantly weaker than that of histologically normal tissue from the same patient [8]. We developed an algorithm to identify histologically abnormal cervix based on comparisons of fluorescence intensities of colposcopically normal biopsies with biopsies to be diagnosed from the same

0090-8258/94 $5.00

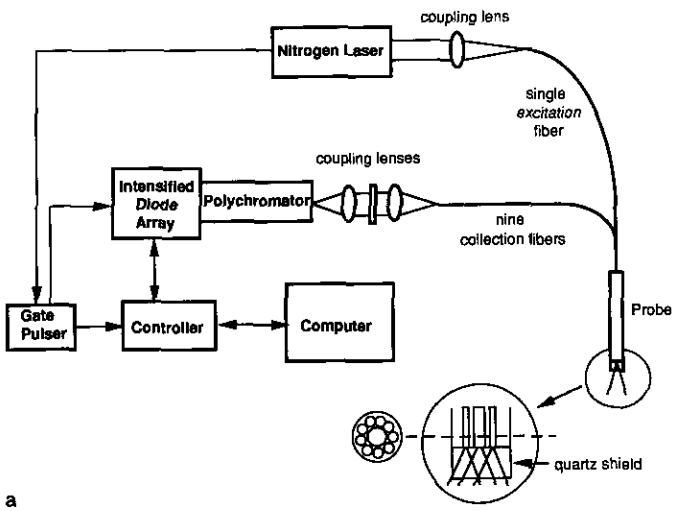

a

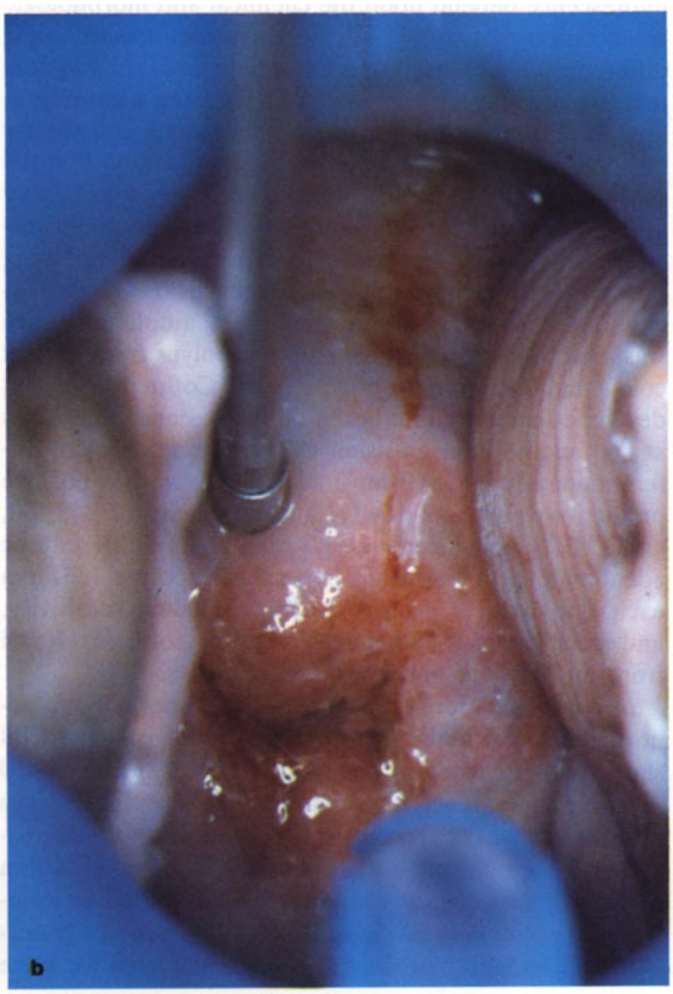

b

FIG. 1. (a) Block diagram of the spectroscopic system used to collect fluorescence spectra of the cervix during colposcopy and (b) photograph displaying the tip of the diagnostic fluorescence probe in contact with the cervix.

patient, obtained at the same time. The positive predictive value, sensitivity, and specificity of this algorithm were 86, 88, and 75%, respectively.

Based on the encouraging diagnostic potential of fluorescence spectroscopy and capability to measure tissue fluorescence rapidly and remotely *in vivo*, we designed a clinical study to measure laser induced autofluorescence at 337 nm excitation [8], of the intact cervix at colposcopy. Our goal was to develop and evaluate the performance of a spectroscopic method to differentiate CIN from normal and nonneoplastic abnormal cervical tissues.

MATERIALS AND METHODS

A spectroscopic system incorporating a pulsed nitrogen laser, an optical fiber probe, and an optical multichannel analyzer was utilized to record fluorescence spectra of the cervix *in vivo* (Fig. 1a). The diagnostic probe is a flexible fiber bundle, which has two legs; one contains a single large fiber (0.22 Numerical Aperture (NA), 200 μm core diameter) and the other contains nine smaller fibers (0.22 NA, 100-μm core diameter). The two legs merge to form a common bundle, which is enclosed in a rigid aluminum jacket (3 mm outer diameter). The large fiber, which is centrally placed, delivers excitation light to the tissue surface and the nine surrounding fibers collect tissue fluorescence only from the surface area directly illuminated by the excitation light. The tip of the probe is shielded with a quartz optical flat, 3 mm in diameter and 2 mm thick. The purpose of this shield is to provide a fixed distance between the tissue and the fibers, so fluorescence intensity can be reported in calibrated units.

Excitation light from the nitrogen laser (Laser Photonics, LN300C) is focused via a quartz lens into the distal end of the central fiber, producing a 1-mm-diameter spot at the outer face of the shield. The laser characteristics for this study were 337-nm wavelength, 5-ns pulse duration, 40-Hz repetition rate, and a transmitted pulse energy of 70 μJ. The distal ends of the nine emission collection fibers were arranged in a circular array and imaged at the entrance slit of a polychromator (Jarrell Ash, Monospec 18) to disperse the fluorescence as a function of wavelength. Fluorescence intensities were recorded using an intensified 1024-diode array controlled by a multichannel analyzer (Princeton Instruments, OMA). A 370-nm long-pass filter was used to block any scattered excitation light from the detector. A 205-ns collection gate, synchronized to the leading edge of the laser pulse using a pulser (Princeton Instruments, PG200), effectively eliminated the effects of the colposcope's white-light illumination during fluorescence measurements. Data acquisition was computer controlled.

The patients examined with this spectroscopic system were selected from a group of patients referred for col-

poscopy for suspected CIN on the basis of abnormal cervical cytology. Informed consent was obtained from each patient and the study was reviewed and approved by the Internal Review Boards of the University of Texas at Austin and the University of Texas M.D. Anderson Cancer Center. Each patient underwent repeat Papanicolon smear and placement of 6% acetic acid to the cervix. Using the colposcope, abnormal areas were identified. Before biopsy, the rigid end of the diagnostic probe was inserted into the vagina under colposcopic control, until the tip was in contact with the tissue surface, and then fluorescence spectra were acquired (Fig. 1b). On average, spectra from two abnormal sites and two normal sites were obtained. All normal spectra were acquired from the squamous epithelium of the ectocervix. Abnormal spectra were acquired from areas surrounding the boundaries of the squamocolumnar junction. Biopsies were taken only from the abnormal sites at the same areas examined spectroscopically by the probe (± 1 mm). Biopsies were not obtained from colposcopically normal sites to comply with routine patient care procedures. Histologic examination of the biopsies was performed using the standard diagnostic classification scheme [9] by a gynecologic pathologist (E. S.).

Prior to each patient study the probe was disinfected and fluorescence intensity of a rhodamine calibration standard was recorded. The probe was disinfected with Metricide (Metrex Research Corp.). As this solution is highly fluorescent, the probe was thoroughly rinsed following disinfection. A background spectrum was then recorded with the tip of the probe immersed in distilled water. This background verified no evidence of trace disinfectant and was automatically subtracted from all subsequently acquired data. The probe was dipped in distilled water and then placed on the face of a quartz cuvette containing a standard rhodamine solution (2 mg/liter in ethylene glycol) and five spectra were measured. After calibration, fluorescence spectra were acquired from the cervix. Fifteen spectra were obtained from each cervical site, which required a total of 375 ms. The probe was dipped in distilled water before measurement from each cervical site. Fluorescence emission spectra were collected in the visible region of the electromagnetic spectrum from 350 to 700 nm with a resolution of 5 nm (full width at half-maximum). No appreciable photobleaching was observed between the collection of the initial and final spectra of the rhodamine standard or the cervical sites.

In each patient, the cervical spectra ($n = 15$) were averaged to obtain a single spectrum per site. The rhodamine spectra were also averaged. The average spectrum from each cervical site was divided by the peak fluorescence intensity of the average rhodamine spectrum for that patient and absolute fluorescence intensities are reported in these calibrated units. In two patients, the peak intensity of the cervical spectra exceeded the dynamic range of the detector. An attenuation filter (0.3 optical density (OD)) was used to reduce the energy transmitted to the tissue and the measurements were repeated. The corresponding rhodamine spectra and background spectrum were also acquired using the 0.3-OD filter. All spectra were corrected for the nonuniform spectral response of the detection system using correction factors obtained by recording the spectrum of a calibrated tungsten ribbon filament lamp (Model 550C, Optronics Laboratories).

Spectra were collected from 28 patients, from a total of 66 colposcopically normal areas and 49 histologically abnormal areas (5 pathologic inflammation, 21 HPV infection, 9 CIN I, 10 CIN II, 4 CIN III). In this study, all biopsies characterized as having HPV infection demonstrated koilocytosis and nuclear abnormalities that relate to the cytopathic changes associated with HPV. Most of the biopsies also demonstrated epithelial proliferation associted with flat condyloma. In cases where biopsies had multiple diagnoses, the classification of that sample was based on the most severe pathologic finding for the purpose of data analysis. For example, if a biopsy was diagnosed as having CIN II and HPV infection, the pathology of the biopsy was classified as CIN II. All abnormal tissues contained only squamous epithelium with the exception of three biopsies which contained both endocervical and squamous mucosa. Of these three samples, two had CIN I and one had CIN II. In each patient, the colposcopically normal sites interrogated spectroscopically were all within the ectocervix, which contains only squamous epithelium. No biopsies were removed for histologic evaluation from these sites. For the purpose of this initial clinical trial, it was assumed that all colposcopically normal tissues were histologically normal. In the *in vitro* study by Mahadevan *et al.* [8], in which biopsies were obtained from 10 colposcopically normal areas, 8 were normal by histologic examination while 2 contained pathologic inflammation.

RESULTS

Figures 2a and 2b display normal and abnormal cervical spectra from two typical patients. Fluorescence intensities are reported in the same set of calibrated units. In both patients, the fluorescence intensities of histologically abnormal tissues are lower than those of corresponding colposcopically normal tissues. Evaluation of abnormal tissue spectra within a patient indicates that tissues with HPV infection are less fluorescent than tissues with chronic inflammation (Fig. 2a). Tissues with dysplastic changes have a fluorescence intensity lower than that of tissues with HPV infection, with CIN III exhibiting the weakest fluorescence intensity (Fig. 2b).

Spectral lineshapes of normal tissues vary both from

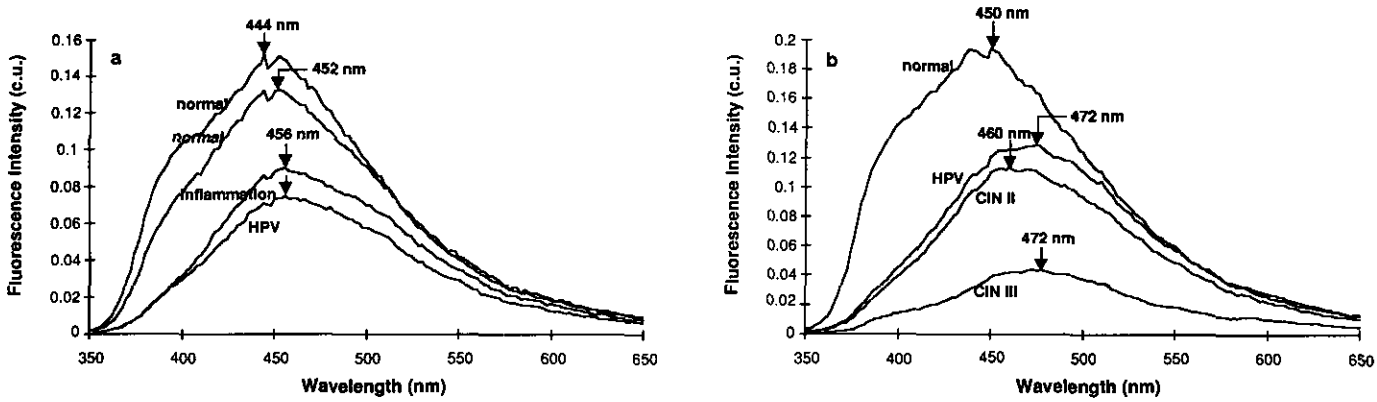

FIG. 2. Fluorescence emission spectra of cervical tissues from (a) a patient with chronic inflammation and HPV infection and (b) a patient with CIN II, CIN III, and HPV infection. Fluorescence intensities are reported in calibrated units.

patient to patient and within a patient (Figs. 2a and 2b). The wavelengths corresponding to the peak intensity of normal tissues occur within ±3 nm of either 442 or 453 nm. A similar phenomenon is observed in the fluorescence lineshapes of abnormal tissues, where peak emission wavelengths occur within ±3 nm of either 444, 454, 464, or 470 nm. The differences in peak emission wavelength between normal and abnormal spectra imply differences in spectral lineshape. One measure of spectral lineshape is the slope of the spectrum over a given wavelength range. It was iteratively determined that the slopes of normal and abnormal spectra were most different from 420–440 nm. At this wavelength range, the slopes of normal spectra were less than those of abnormal spectra,

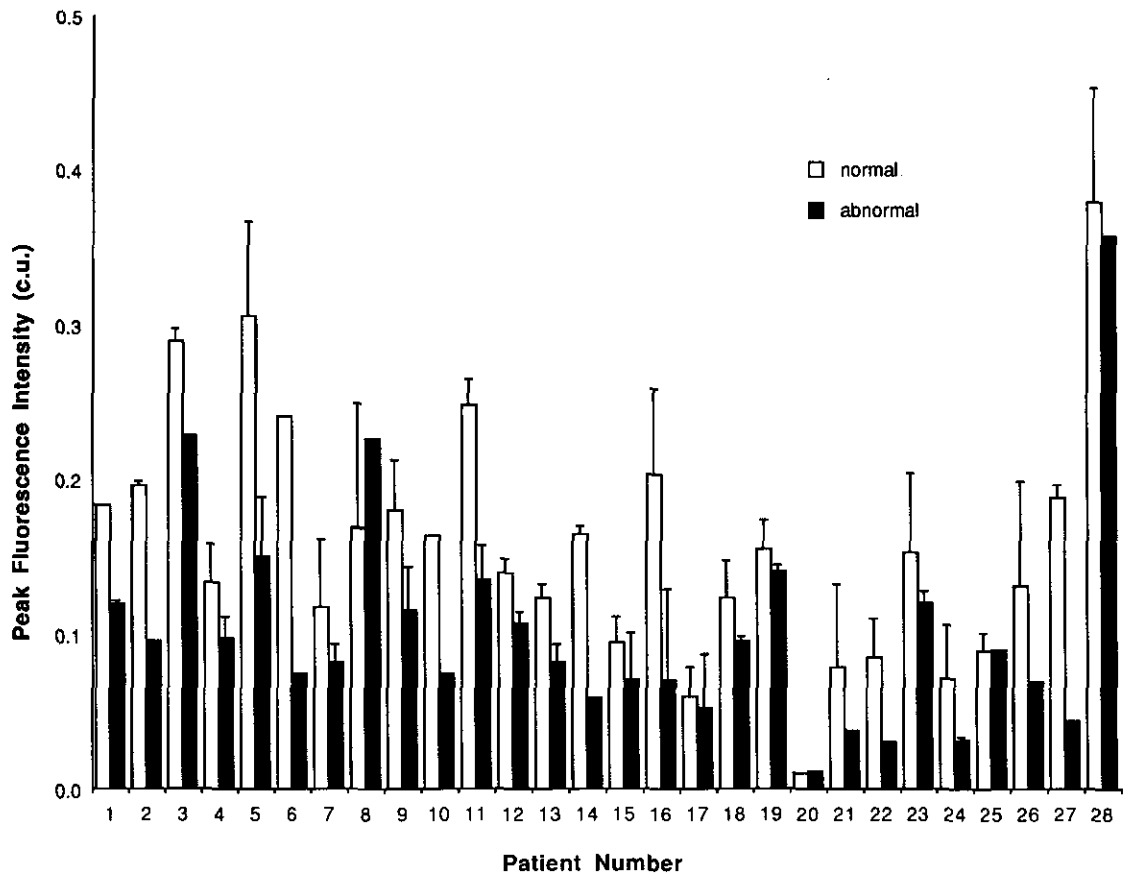

FIG. 3. Bar chart displaying average peak fluorescence intensities of spectra from colposcopically normal (white) and histologically abnormal (black) tissues from 28 patients. The error bars represent one standard deviation. Fluorescence intensity is reported in calibrated units.

TABLE 1
Results of Paired *t* Test Analysis of Peak Fluorescence Intensities

Null hypothesis	Alternate hypothesis	Number of paired samples	Reject null hypothesis with level of significance
Average normal = inflammation	Average normal > inflammation	5	$P < 0.005$
Average normal = HPV	Average normal > HPV	22	$P < 0.001$
Average normal = CIN	Average normal > CIN	23	$P < 0.0005$
HPV = CIN	HPV > CIN	9	$P < 0.05$

reflecting the longer peak emission wavelengths of abnormal tissue spectra.

Figure 3 displays the average peak fluorescence intensity of normal and abnormal spectra from all 28 patients. Fluorescence intensities are reported in calibrated units. In patients with spectra from more than one normal or abnormal site, the error bars represent one standard deviation. The average peak fluorescence intensity of normal tissues varies by more than a factor of five from patient to patient, while generally within a single patient, the standard deviation is less than 25% of the average value. The significant interpatient variations in the average peak fluorescence intensities of normal tissues imply that the peak fluorescence intensities of normal and abnormal tissues need to be analyzed in a paired manner. A paired comparison of the average peak fluorescence intensities of colposcopically normal and histologically abnormal tissues from the same patient indicates that the intensity of abnormal tissues is lower (with the exception of Patients 8, 20, and 25).

To determine whether the peak fluorescence intensities of abnormal tissues are statistically less than the average peak intensity of corresponding colposcopically normal tissues from the same patient, a standard one-sided paired *t* test was employed [10]. The paired *t* test analysis was extended a step further to determine if there were any statistically significant differences between the intensities of the histologically abnormal tissues. Table 1 contains the results of this analysis. The hypothesis that the average peak fluorescence intensity of normal tissues is higher than that of abnormal tissue from the same patient was found to be true below the 0.005 level of significance. The hypothesis that tissues with HPV infection have a higher fluorescence intensity than tissues with CIN from the same patient was found to be true, below the 0.05 level of significance. There was insufficient data in this initial clinical trial to compare peak intensities of tissues with pathologic inflammation to peak intensities of tissues with CIN or HPV infection, or to compare data within the CIN categories.

To determine whether the slopes over the wavelength range 420–440 nm of abnormal tissues are statistically greater than those of corresponding colposcopically normal tissues, a standard one-sided paired *t* test was employed [10]. Prior to extracting the slope, all spectra were normalized to a peak intensity of one. In this paired test the slope of each abnormal sample was compared to that of each normal sample within a given patient. Table 2 contains the results. The hypothesis that the slope over the wavelength range 420–440 nm of abnormal tissues (pathologic inflammation, HPV infection, and CIN) is higher than that of normal tissues was found to be true below the 0.005 level of significance. Significant differences in slope were not observed between tissues with pathologic inflammation, HPV infection, and CIN.

An algorithm was developed to determine whether an unknown *in vivo* tissue site was histologically abnormal based on two spectroscopic components: (1) a paired comparison of the peak fluorescence intensity of the unknown tissue to the average peak intensity of colposcopically normal tissues from the same patient and (2) the slope of the unknown spectrum over the wavelength range of 420–440 nm [11]. This information is represented for all 116 samples as a two-dimensional scatter plot as shown

TABLE 2
Results of Paired *t* Test Analysis of Slope over the Wavelength Range 420–440 nm

Null hypothesis	Alternate hypothesis	Number of paired samples	Reject null hypothesis with level of significance
Normal = inflammation	Normal < inflammation	11	$P < 0.0005$
Normal = HPV	Normal < HPV	49	$P < 0.005$
Normal = CIN	Normal < CIN	49	$P < 0.001$

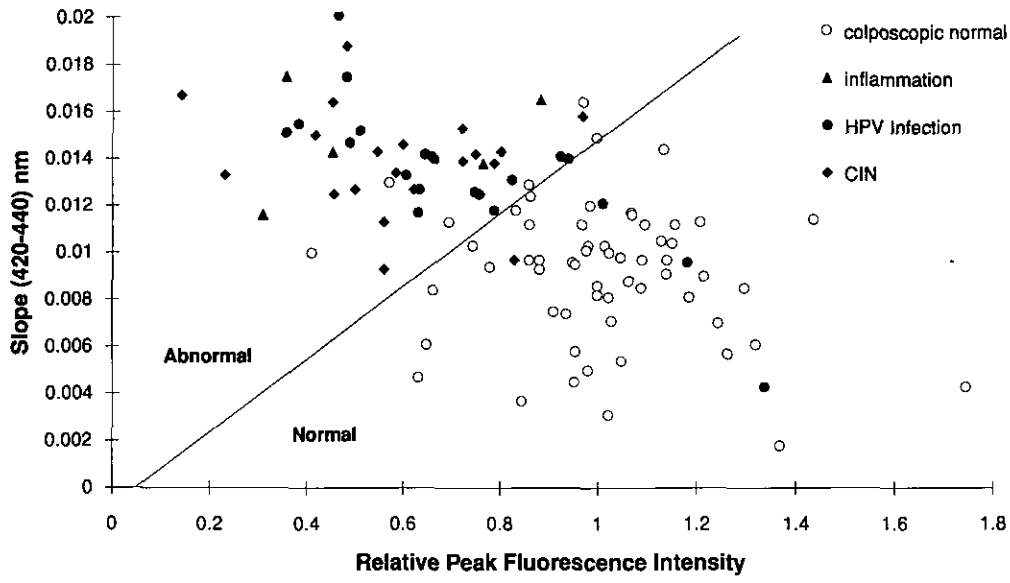

FIG. 4. Two-dimensional scatter plot of the relative peak fluorescence intensity versus the slope over 420 to 440 nm of colposcopically normal (white) and histologically abnormal (black) spectra. The peak fluorescence intensities of all spectra are normalized to the average peak intensity of colposcopically normal spectra from the same patient. The straight line represents the decision surface chosen to minimize the number of misclassified samples.

in Fig. 4. The ordinate corresponds to the slope of each sample over 420 to 440 nm for spectra normalized to a peak intensity of one. The abscissa corresponds to the relative peak fluorescence intensity of each specimen, that is, the peak intensity of each sample divided by the average peak intensity of corresponding colposcopically normal samples from the same patient. The scatter plot was divided into two regions corresponding to normal and abnormal tissues using a straight line decision surface chosen to minimize the number of misclassified samples. The algorithm differentiated histologically abnormal tissues from colposcopically normal tissues with a sensitivity, specificity, and positive predictive value of 92, 90, and 88%.

A positive correlation was observed between the peak emission wavelength of CIN spectra and the peak emission wavelength of normal spectra from the same patient. For example, if the peak emission of the normal tissue occurs at 444 nm, the corresponding CIN sample from the same patient peaks near 454 nm. If the normal spectrum peaks at 450 nm, then the corresponding CIN sample from the same patient peaks near 460 nm. A similar correlation was not observed for samples with inflammation and HPV infection. This provided the basis for a preliminary diagnostic algorithm to differentiate CIN from tissues with HPV infection or pathologic inflammation within a single patient [11]. This algorithm correctly diagnosed CIN with a sensitivity of 87%, a specificity of 73%, and a positive predictive value of 74%.

Table 3 lists the sensitivities, specificities, and positive predictive values of the two diagnostic algorithms as well as that of colposcopy [8]. Spectroscopic diagnosis using Algorithm (1) differentiates histologically abnormal tissues from colposcopically normal tissues (Fig. 4), and spectroscopic diagnosis using Algorithm (2) differentiates CIN from HPV infection and pathologic inflammation. The sensitivity, specificity, and positive predictive value of Algorithm (1) are similar to those of colposcopy for diagnosing histologically abnormal tissues from those that are colposcopically normal.

DISCUSSIONS AND CONCLUSIONS

This study indicates the potential of laser-induced fluorescence at 337 nm excitation to improve colposcopic detection of CIN. Unlike conventional colposcopy, spectroscopic diagnosis has the ability to differentiate neoplastic (CIN) and nonneoplastic abnormal lesions (pathologic inflammation, HPV infection) of the cervix. Tissue fluorescence can be measured rapidly and remotely *in vivo*, permitting real-time diagnosis, and algorithms can be implemented in software, placing automated cancer detection in the hands of less experienced practitioners. We speculate that these inherent advantages of fluorescence spectroscopy may aid in reducing the mortality rate of cervical carcinoma by providing more effective patient management and wide-scale implementation of precancer and cancer diagnosis.

TABLE 3
Sensitivity, Specificity, and Positive Predictive Values of Colposcopy and the Spectroscopic Algorithms

Diagnostic method	Sensitivity (%)	Specificity (%)	Positive predictive value (%)
Colposcopic diagnosis of histologically abnormal cervical tissue	78	89	88
Spectroscopic diagnosis of histologic abnormality using Algorithm (1)	92	90	88
Spectroscopic diagnosis of CIN using Algorithm (2)	87	73	74

Before the technique can be implemented clinically, a number of important issues must be addressed. Future studies with larger numbers of patients will be conducted to evaluate the performance of the spectroscopic algorithms developed in this initial study. Particularly, spectra will be acquired from a large group of patients with HPV infection, pathologic inflammation, and CIN to substantiate the performance of the second algorithm that differentiates tissues with CIN from those with HPV infection and those with inflammation. Furthermore, a large group of patients with various grades of CIN lesions, microinvasive carcinoma, and early invasive carcinoma will also be spectroscopically interrogated. These data will be analyzed to determine if an algorithm to differentiate between CIN I, CIN II, CIN III carcinoma *in situ* and invasive carcinoma can be developed.

Three factors can be identified which may contribute to the interpatient variations and in some cases intrapatient variations in the peak fluorescence intensities of normal and abnormal tissues. Differences in the distribution of fluorophores from one sample to another will lead to variations in detected fluorescence. A second contributing factor may be the fact that our study included data from abnormal samples with multiple diagnoses. For instance, tissues were classified as CIN even if they contained inflammation or evidence of HPV infection in addition to dysplastic changes. Finally, variations in lesion size may contribute to this variability. In some cases, the 1-mm-diameter spot interrogated by the probe was significantly larger than small, localized abnormal lesions such as focal CIN. In future studies, with larger numbers of patients, we will investigate the feasibility of differentiating samples with single histologic abnormalities from those with multiple histologic abnormalities. In addition, we will correlate our signals with the size and depth of the dysplastic lesion. To understand other contributions to interpatient as well as intrapatient variations in tissue spectra, correlation studies will be performed between the spectroscopy of the normal cervix and the physiologic state of the cervix, such as stage in menstrual cycle, gestational history, previous history of cervical trauma, and age.

In summary, the initial success of the spectroscopic diagnosis of CIN *in vivo*, coupled with the ease with which the technique can be implemented, suggests the potential of using this technique as a tool for diagnosing cervical intraepithelial neoplasia. Extensive studies, however, are required to understand and uniquely classify the pathologic variations of the cervix. Using a combination of fluorescence microscopy and microspectrofluorimetry, we will investigate the biochemical and morphologic origin of the spectral differences between the normal and various histologically abnormal cervical tissues. This will provide greater insight into the physical mechanisms that lead to the changes in autofluorescence observed in neoplasia.

We speculate that if algorithms with sufficient sensitivity and specificity to differentiate between the clinically significant pathologies of the cervix can be developed, fluorescence spectroscopy can circumvent the need for biopsy and pathologic analysis. Potentially, this may allow combined diagnosis and therapy in a single office visit.

ACKNOWLEDGMENT

Financial support from the Whitaker Foundation is gratefully acknowledged.

REFERENCES

1. Beral, V. Prediction of cervical cancer incidence and mortality in England and Wales, *Lancet* **1,** 495 (1986).
2. Koss, L. G. The Papanicolaou test for cervical cancer detection, *J. Am. Med. Assoc.* **261,** 737–743 (1989).
3. Gay, J. D., Donaldson, L. D., and Goellner, J. R. False negative results in cervical cytologic studies, *Acta Cytol.* **29,** 1043–1046 (1985).
4. Burke, L., Antonioli, D. A., and Ducatman, B. S. *Colposcopy, text and atlas,* Appleton and Large, Norwalk, CT (1991).
5. Lam, S., Hung, J. Y. C., Kennedy, S. M., Leriche, J. C., Vedal, S., Nelems, B., Macaulay, C. E., and Palcic, B. Detection of dysplasia and carcinoma in situ by ratio fluorometry, *Am. Rev. Respir. Dis.* **146,** 1458–1461 (1992).
6. Cothren, R. M., Richards-Kortum, R. R., Sivak, M. V., Fitzmaurice, M., Rava, R. P., Boyce, G. A., Hayes, G. B., Doxtader, M., Blackman, R., Ivanc, T., Feld, M. S., and Petras, R. E. Gastrointestinal tissue diagnosis by laser induced fluorescence spectroscopy at endoscopy, *Gastrointest. Endosc.* **36,** 105–111 (1990).
7. Schomaker, K. T., Frisoli, J. K., Compton, C. C., Flotte, T. J., Richter, J. M., Nishioka, N. S., and Deutsch, T. F. Ultraviolet

laser-induced fluorescence of colonic tissue: Basic biology and diagnostic potential, *Lasers Surg. Med.* **12,** 63–78 (1992).

8. Mahadevan, A., Mitchell, M. F., Silva, E., Thomsen, S., and Richards-Kortum, R. R. A study of the fluorescence properties of normal and neoplastic human cervical tissue, *Lasers Surg. Med.,* in press (1993).
9. Ferenczy, A. Cervical intraepithelial Neoplasia, in *Pathology of the female genital tract* (A. Blaustein, Ed.), Springer-Verlag, New York, pp. 156–177 (1982).
10. Walpole, R. E., and Meyers, R. H. *Probability and statistics for engineers and scientists,* Macmillan, New York (1978).
11. Ramanujam, N., Mitchell, M. F., Mahadevan, A., Thomsen, S., and Richards-Kortum, R. R. *In vivo* diagnosis of cervical intraepithelial neoplasia (CIN) using 337 nm excited laser induced fluorescence, submitted for publication.